Effect of static charges on mechanical-to-electrical energy conversion of electrospun PVDF nanofiber mats

Hao Shao, Jian Fang, Hongxia Wang, Tong Lin*

Institute for Frontier Materials, Deakin University, Geelong, VIC 3216, Australia

*Corresponding author. Tel : (+61) 3 52271245; E-mail: tong.lin@deakin.edu.au

Received: 17 October 2016, Revised: 15 November 2016 and Accepted: 21 November 2016

DOI: 10.5185/amlett.2017.1461
www.vbripress.com/aml

Abstract

Polyvinylidene fluoride (PVDF) nanofiber mats prepared using electrospinning technique have been used for making mechanical-to-electrical energy conversion devices. However, the effect of residual charges on this energy conversion process has never been seriously considered yet. In this study, by removing residual charges from electrospun PVDF nanofiber mats using a solvent treatment method, the contribution of the charges to device energy harvesting performance was carefully examined. It has been found that isopropanol treatment could effectively remove most of residual charges from the nanofiber mats, without obviously affecting crystal structure of the fibers. The electric outputs decreased from 1.0 V and 1.2 μA to 0.45 V and 0.5 μA after the residual charges removal. It can be concluded that residue charges play an important role in mechanical-to-electrical energy conversion of electrospun nanofibers. The understanding obtained from this study may supply a strategy for enhancing electric outputs of piezoelectric devices in future.

Keywords: PVDF, electrospinning, static charge, piezoelectric.

Introduction

As a typical piezoelectric polymer, polyvinylidene fluoride (PVDF) has been widely used in making mechanical-to-electrical energy conversion devices including energy harvesters, actuators, transducers and sensors [**1-3**]. PVDF is a semi-crystalline polymer with the monomer unit of -CH_2CF_2- [**4**]. It has five different crystal phases, i.e. α, β, γ, δ and ε, related to different chain conformations [**5**], with the α and β phases being mostly examined in the literature. The non-polar TGTG' (trans-gauche-trans-gauche) structure of α phase shows the most thermodynamical stability, while β phase with all trans (TTTT) planar zigzag structure has the highest dipolar moment per unit which contributes to excellent pyroelectric, ferroelectric and piezoelectric properties of PVDF [**6**]. High β crystal phase content in PVDF is highly desirable for mechanical to electric energy conversion.

Traditionally, piezoelectric PVDF film is prepared by a complicated process including physically stretching a PVDF film, to convert the α phase into the β phase, and subsequently poling in a high electric field at an elevated temperature to make the dipole moment align in a specific direction [**7**]. Considerable efforts have been devoted to enhancing β crystal phase content through adjusting fabrication condition, adding functional fillers and blending PVDF with other polymers [**5, 8-10**].

Recently, using electrospinning to prepare piezoelectric PVDF nanofibers has been reported by our and other research groups [**1**, **4**, **7**, **11**]. Electrospinning is an efficient method to prepare polymer nanofibers. It involves drawing a polymer fluid into solid nanofibers under a high electric field [**12**]. In most cases, the fibers are collected in the form of randomly orientated non woven fibrous mats. When a PVDF solution is electrospun, the resulting nanofibers already contain a high β phase content and electrospun PVDF nanofiber mats showing excellent piezoelectricity and mechanical-to-electrical energy conversion property, through without extra poling treatment. A thin electrospun PVDF nanofiber mat can generate several volts of voltage outputs under a compressive pressure. For instance, Jian *et al.* reported that electrospun PVDF nanofiber membranes could generate electric output of several volts under mechanical compression, which was much higher than that of commercial piezoelectric PVDF film [**1**]. Hao *et al.* also indicated that the electric outputs of electrospun PVDF nanofiber mats were highly affected by electrospinning parameters [**7**].

The electricity generated from the nanofiber mat can be easily stored in a capacitor to power various microelectronic devices [**1**, **13**, **14**]. Such an energy conversion behavior comes from the simultaneous effects of mechanical stretching and electrical poling during electrospinning process [**15**]. Such an energy conversion feature was attributable to the high-ratio stretching applied to the solution jet and the orientation of dipole in the polymer chains.

It has been established that electrostatic charges are trapped within nanofibers during electrospinning [**16**, **17**], though the collector is grounded. Because of the insulating feature of polymer nanofibers, the charges carried by electrospun nanofibers can stay stably for a long time in an ambient condition. During the compression process of PVDF nanofiber mats, mat deformation could lead to imbalance of the electric charges and generate signals that should be differentiated from piezoelectric signals generated by the nanofibers. However, the role of the residual charges in PVDF nanofibers on their mechanical to electricity conversion property has not been reported in the research literature. Understanding the effect of residual charges on the energy conversion would assist in clarifying the power generation mechanism of electrospun nanofiber mats.

In this study, we examined the effect of residual charges on the mechanical-to-electrical energy conversion of PVDF nanofiber mats. By removing the charges through treatment in an organic solvent, we showed that the residue charge play an important role in mechanical to electricity conversion. The device made of as-spun PVDF nanofiber mat could generate approximately 1.0 V voltage and 1.2 μA current outputs with the residue charge level of -0.018 nC/cm^2, whereas after removing the charges, the device showed reduced electric outputs, 0.45 V and 0.5 μA. In this study, we for the first time prove the role of electrostatic charge in electrospun nanofibers for mechanical to electrical conversion. It would assist to enhance our understanding on this novel material and development of nanofiber energy harvesting devices.

Experimental

Materials

PVDF pellets (Mw=275,000), N, N-dimethylformamide (DMF), acetone and isopropanol (anhydrous, 99.5%) were purchased from Sigma-Aldrich and used as received.

Electrospinning

The 20% (w/v) PVDF solution was prepared by dissolving PVDF pellets into DMF/acetone (v/v 4/6) mixture solvent at 70 °C. For electrospinning, the PVDF solution was placed in a 5 mL plastic syringe which was fitted with a steel needle (21G size). A high voltage of 15 kV was applied to the steel needle by a positive DC power supply (Gamma High Voltage) while the flow rate was controlled at 1.0 mL/h by a syringe pump (KD Scientific). The spinning distance was set at 15 cm and a grounded aluminum rotating drum (length: 10 cm; diameter: 5 cm; rotating speed: 100 rpm) was used as a collector to collect nanofibers. The thickness of fiber mats was controlled at 100 μm by adjusting the fiber deposition time.

Static charge removal

Electrostatic charges were removed from electrospun PVDF nanofibers according to the method specified in a standard (EN 779: 2002). In details, the nanofiber mat was immersed in isopropanol for a certain period of time and then dried on a grounded metal substrate. These treatments were carried out in a fume hood at room temperature.

Characterizations

The morphology of PVDF nanofiber mats was observed by a scanning electron microscopy (SEM, Zeiss Supra 55VP). The specimen was gold-coated by sputter coating prior to SEM observation (LEICA EM ACE600). Fiber diameter was measured using an image processing software Image J based on the SEM images. X-ray diffraction (XRD) pattern was recorded on a Panalytical X-ray diffraction using Cu Kα radiation (1.54Å). Flourier transform infrared (FTIR) spectroscopy was collected using a Bruker Optics spectroscopy. The specimen was put on top of the ATR set and scanned from 1350 to 650 cm^{-1}. Differential scanning calorimetry (DSC) was performed on TA Q200 machine heating from 25 °C to 200 °C at the rate of 10 °C/min in nitrogen atmosphere. The thickness of the PVDF nanofiber mats was measured by a digital micrometer. The residue charge level of nanofiber mats was measured using a Keithley 6514 meter. In details, a copper container was placed in a grounded metal box which provided electromagnetic shielding during measurement. A polyester plate was used to separate the copper container and metal box. When a piece of PVDF nanofiber mat was put in the copper container, the residue charge value was measured by the equipment. The mechanical-to-electrical energy conversion properties were characterized using a purposed built testing platform reported previously [**1**]. The compression force was 10 N while the frequency was controlled at 1 Hz.

Results and discussion

Fig. 1(a) shows the SEM image of the electrospun PVDF nanofibers. All fibers are randomly-oriented. They look uniform in morphology without beads. The average diameter was about 300 nm. The crystal structure of the PVDF nanofibers was investigated through XRD analysis and FTIR spectroscopy, as shown in **Fig. 1b** and **1c**. An intensive peak at around 2θ = 20.6º can be observed in XRD pattern which corresponds to the (110) and (200) planes, confirming the predominating β crystal phase of the electrospun PVDF nanofibers [**7**, **18**, **19**]. The tiny peak at 18.4º was assigned to the (020) diffraction plane of α phase. The FTIR spectroscopy showed lots of vibration peaks, associated with α, β, γ crystal phases and amorphous phase of PVDF. The peaks at 761, 870 and 970 cm^{-1} were assigned to the α crystal phase, while the peaks at 840 and 1278 cm^{-1} to the β crystal phase [**20-22**].

FTIR result is commonly used for quantifying the α and β crystal phase contents of PVDF materials [**7**, **23**]. Assuming FTIR absorption peaks follow the Lambert-Beer law with the absorption coefficients of K_α (6.1×10^4 cm^2 mol^{-1}) and K_β (7.7×10^4 cm^2 mol^{-1}) at the wavenumber of 761 and 840 cm^{-1}, respectively, the β crystal phase content in the PVDF nanofibers can be estimated according to the equation (1) [**7**, **23**]:

$$F(\beta) = \frac{X_\beta}{X_\alpha + X_\beta} = \frac{A_\beta}{(K_\beta/K_\alpha)A_\alpha + A_\beta} = \frac{A_\beta}{1.26A_\alpha + A_\beta} \quad (1)$$

where, $F(\beta)$ is the β crystal phase content; X_α and X_β represent the crystalline mass fractions of the α and β crystal phases, while A_α and A_β are the absorbance at 761 cm^{-1} and 840 cm^{-1}, respectively. Based on this equation, the β crystal phase content in PVDF nanofibers was calculated at about 85.3%, which confirms that β crystal phase is the predominant phase in the nanofibers.

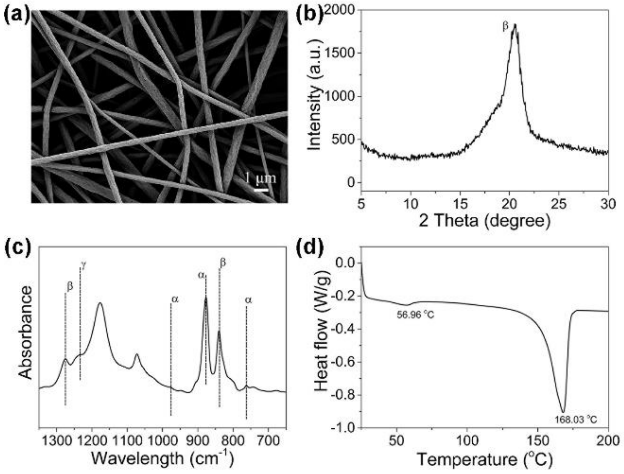

Fig. 1. (a) SEM image, (b) XRD pattern, (c) FTIR spectra and (d) DSC result of electrospun PVDF nanofibers.

Fig. 1d shows the DSC curve of PVDF nanofibers. Two endothermic peaks were observed, involving the glass transition endothermic peak at about 57 °C and melting endothermic peak at around 168 °C. The degree of crystallinity (ΔX_c) was calculated by the following equation (2) [**24**]:

$$\Delta X_c = \frac{\Delta X_m}{\Delta X_{100}} = \frac{\Delta X_m}{x\Delta X_\alpha + y\Delta X_\beta} \quad (2)$$

Here, ΔX_m is the melting enthalpy of the PVDF nanofibers while ΔX_{100} is the melting enthalpy of a 100% crystalline PVDF. ΔX_α and ΔX_β represent the melting enthalpies of a 100% crystalline PVDF of α and β crystal phases. x and y are the amount of α and β crystal phase contents in PVDF nanofibers, respectively. In this study, the value of ΔX_α and ΔX_β were 93.07 J/g and 103.4 J/g, respectively. The coefficients of x and y were obtained previously from FTIR result about 14.7% and 85.3%. After calculation, the crystallinity was approximately 47%.

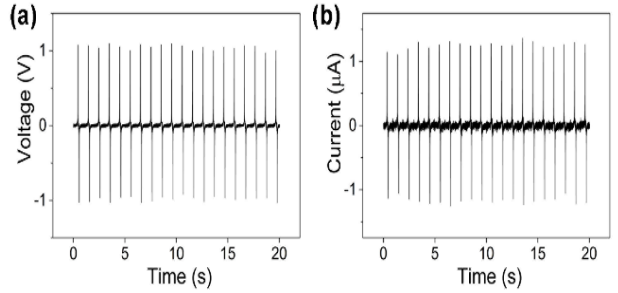

Fig. 2. (a) Voltage and (b) current outputs of the device prepared by as-spun PVDF nanofiber mat. (Thickness: 100 μm; working area: 4 cm^2.)

The mechanical-to-electrical energy conversion property of the as-spun PVDF nanofiber mats was measured. When a periodic compression was applied to the nanofiber device, the electric signals were recorded, as shown in **Fig. 2**. Each compression impact resulted in two output signals with opposite polarities related to compressive deformation and deformation recovery [**1**]. The repeated impact led to an alternating current (AC) output, which is typical for piezoelectric devices. Under the experimental condition, the device generated a stable voltage output of 1.0 V and current output of 1.2 μA.

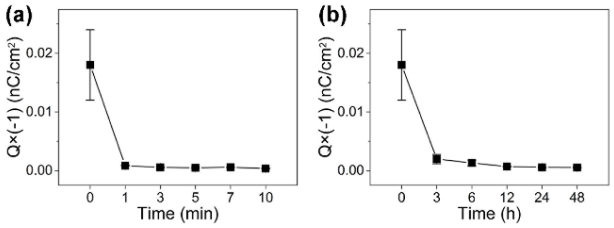

Fig. 3. Effect of (a) isopropanol immersion time (post drying, 24 hours) and (b) post drying time (isopropanol treatment, 3 minutes) on the residual charge of the PVDF nanofiber mats.

To examine the effect of residual charges on mechanical-to-electrical energy conversion, we used a solvent to remove electrostatic charges from the PVDF nanofibers. To do this, nanofiber samples were immersed in isopropanol for certain period of time at room temperature, and then dried on a grounded metal plate at room temperature. **Fig. 3a** shows the influence of immersion time on the overall residual charges after drying for 24 hours. The electric charges (Q) carried by the as-spun PVDF nanofiber mats were around 0.018 nC/cm^2 with a variation among different mats, probably attributed to the influence of environment humidity and air ventilation during electrospinning [**25**, **26**]. After isopropanol treatment, the electric charge level of the fibers declined dramatically. More than 96% of the residue charges in the fibers were removed after immersing the sample in isopropanol for 1 minute. The removal of electric charges was explained by the polar structure of isopropanol [**27-29**]. A significant charge separation could occur in hydroxyl group, leaving a positive and a negative end.

The residue charges in the fibers can be easily attracted to the positive end of the isopropanol molecule, and they are removed due to the evaporation of the isopropanol [**30**].

Fig. 3b shows the influence of drying time on charge removal after immersing the nanofiber mat in isopropanol for 3 minutes. About 84.2% of the residual charges were removed after drying the isopropanol treated mat for three hours. With the increase in drying time, more residual charges were removed. Drying 24 hour enabled to remove 96.5% charges from the nanofiber samples. Therefore, the immersion in isopropanol for 3 minutes followed by 24 hours drying was chosen to remove residual charges from nanofibers in the following experiments. As β crystal phase in PVDF is critical to its mechanical-to electricity conversion property, the effect of the isopropanol treatment on β crystal phase content was examined.

Fig. 4a shows the FTIR spectra of the original PVDF nanofiber mat and the mats after isopropanol treatment for different periods of time. A negligible effect of isopropanol treatment on the crystal structure was observed.

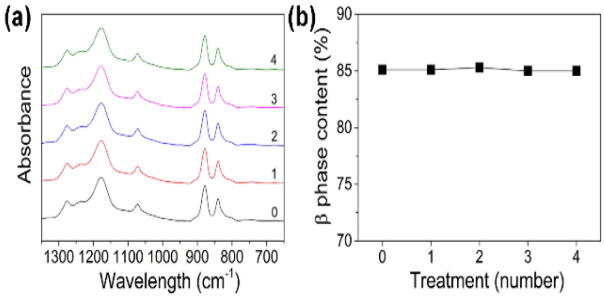

Fig. 4. (a) FTIR spectra and (b) calculated β crystal phase content of PVDF nanofiber mats before and after repeated solvent treatment.

Fig. 5a&b show the mechanical-to-electrical energy conversion performance of PVDF nanofiber mat before and after charge removal. To avoid the generation of extra static charges during compression process, the charge removal treatment was repeated for 4 times. Under repeated compression (force 10 N, frequency 1 Hz). The as-spun PVDF nanofiber mat brought residual charge of -0.018 nC/cm^2, and the device made of such nanofiber sample generated the electric outputs of 1.0 V and 1.2 μA.

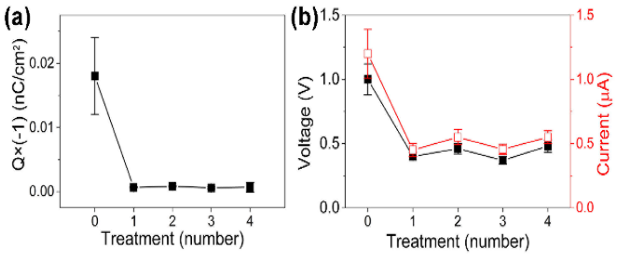

Fig. 5. (a) The residual charge level of PVDF nanofiber mat before and after repeated solvent treatment; (b) voltage and current outputs of PVDF nanofiber mat before and after repeated solvent treatment. (Mat thickness: 100 μm; working area: 4 cm^2.)

After each isopropanol treatment, the residual charges within the nanofiber mat were almost negligible. The device made of this nanofiber sample showed reduction in both voltage and current outputs, to 0.45 V and 0.5 μA, respectively. Further treatment with isopropanol showed no obvious reduction in the electric charge quantity and electric outputs. These results also suggest that isopropanol treatment is an effective method to remove electric charges from electrospun nanofibers.

It is known that electrostatic charges play a significant role in triboelectric energy harvesting [**31**, **32**]. During the mechanical-to-electrical energy conversion process, the residue charges in the nanofiber mat could be polarized due to mechanical deformation of the mat, which contributes to the electric outputs. The result that the nanofiber mat after removal of the residual charges only generates 45% of the electric outputs suggested the important contribution of the charges.

The electric outputs before and after removing the residual charges were compared with previously reports. As shown in **Table 1**, compression frequency played a significant role in mechanical-to-electrical energy harvesting. Electric voltage and current outputs obtained from the compression of 5 Hz were much higher than the values generated from 1 Hz compression frequency, although smaller working area. While the compression frequency and working area were the same, the electric outputs in this work were comparable with the values obtained from the mat with the thickness of 140 μm. The thickness difference should be in the error range of the digital micrometer as the PVDF nanofiber mat had fluffy porous structure and was easily impacted under external compression. In addition, the amount of residual charges inside of 140 μm mat itself was not indicated previously. After charge removal, the electric outputs in this work decreased obviously.

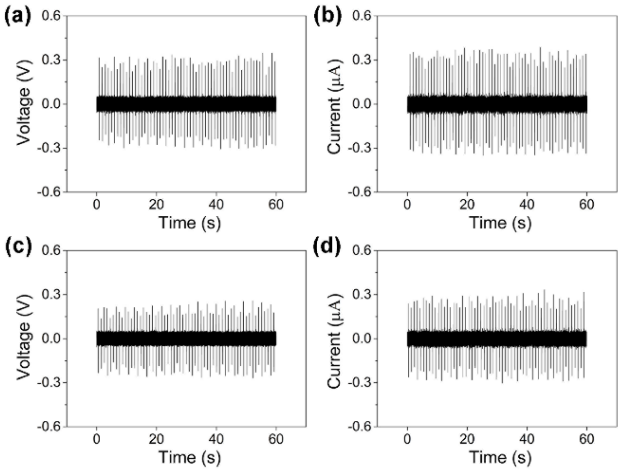

Fig. 6. (a) & (c) Voltage and (b) & (d) current outputs of commercial PVDF film before and after the isopropanol treatment. (Film thickness: 40 μm; working area: 4 cm^2).

For comparison, we also tested the piezoelectricity of commercial piezoelectric PVDF film. The mechanical-to-electrical energy conversion property of commercial

Table 1. The comparison of various electrospun PVDF nanofiber devices.

Devices	Working area (cm^2)	Mat thickness (μm)	Frequency (Hz)	Voltage output (V)	Current output (μA)	Ref.	
1	2	140	5	2.2	3.9	[**1**]	
2	2	100	5	2.6	4.5	[**13**]	
3	4	140	1	1.1	1.2	[**7**]	
4	4	100	1	1.0	1.2	This work	Before charge removal
				0.45	0.5		After charge removal

PVDF film after isopropanol treatment had a little change, from 0.28 to 0.23 V for the voltage output and 0.3 to 0.27 μA for the current outputs (**Fig. 6**). All the values are much lower than these of electrospun PVDF nanofiber mats.

Conclusion

We have examined the role of residual charges on the mechanical-to-electrical energy conversion behavior of electrospun PVDF nanofiber mats. After isopropanol treatment, more than 96% charges can be removed from PVDF nanofibers. This led to decrease of electric outputs, from 1.0 V to 0.45 V (current from 1.2 μA to 0.5 μA). Residual charges should play an important role in mechanical to electric energy conversion. Despite of this, the electric outputs from electrospun nanofiber mat after removal of the residual changes were still higher than those of commercial PVDF piezoelectric films. These new understanding may benefit the future development of nanofiber based energy harvesting devices and mechanical sensors.

Acknowledgements

The authors acknowledge the support from Australian Research Council (ARC) through a Future Fellowship grant (ARC FT120100135).

Author's contributions

Conceived the plan: Tong Lin; Performed the expeirments: Hao Shao; Data analysis: Hao Shao, Jian Fang, Hongxia Wang, Tong Lin; Wrote the paper: Hao Shao, Jian Fang, Tong Lin. Authors have no competing financial interests.

References

1. Fang, J.; Wang, X.; Lin, T.; *J. Mater. Chem.*, **2011**, *21*, 11088. **DOI:** 10.1039/c1jm11445j
2. Zhang, Q.; Lewin, P.A.; Bloomfield, P.E.; *IEEE Trans. Ultrason. Eng.*, **1997**, *44*, 1148. **DOI:** 10.1109/58.655640
3. Seminara, L.; Capurro, M.; Cirillo, P.; Cannata, G.; Valle, M.; *Sens. Actuators, A*, **2011**, *169*, 49. **DOI:** 10.1016/j.sna.2011.05.004
4. Ahn, Y.; Lim, J.Y.; Hong, S.M.; Lee, J.; Ha, J.; Choi, H.J.; Seo, Y.; *J. Phys. Chem. C*, **2013**, *117*, 11791. **DOI:** 10.1021/jp4011026
5. Martins, P.; Lopes, A.; Lanceros-Mendez, S.; *Prog. Polym. Sci.*, **2014**, *39*, 683. **DOI:** 10.1016/j.progpolymsci.2013.07.006
6. Sundaray, B.; Bossard, F.; Latil, P.; Orgéas, L.; Sanchez, J.Y.; Lepretre, J.C.; *Polymer*, **2013**, *54*, 4588. **DOI:** 10.1016/j.polymer.2013.05.049
7. Shao, H.; Fang, J.; Wang, H.; Lin, T.; *RSC Adv.*, **2015**, *5*, 14345. **DOI:** 10.1039/C4RA16360E
8. Mahadeva, S.K.; Berring, J.; Walus, K.; Stoeber, B.; *J. Phys. D: Appl. Phys.*, **2013**, *46*, 285305. **DOI:** 10.1088/0022-3727/46/28/285305
9. Shukla, S. K.; Parlak, O.; Shukla, S. K.; Mishra, S.; Turner, A. P. F.; Tiwari, A., *Industrial & Engineering Chemistry Research*, **2014**, 53, 8509.
10. Abdullah, I.Y.; Yahaya, M.; Jumali, M.H.H.; Shanshool, H.M.; *Opt. Quantum Electron.*, **2016**, *48*, 1. **DOI:** 10.1007/s11082-016-0433-1
11. Sharma, M.; Srinivas, V.; Madras, G.; Bose, S.; *RSC Adv.*, **2016**, *6*, 6251. **DOI:** 10.1039/C5RA25671B
12. Reneker, D.H.; Yarin, A.L.; Zussman, E.; Xu, H.; Advances in Applied Mechanics; Elsevier: Netherlands, **2007**. **DOI:** 10.1016/S0065-2156(07)41002-X
13. Ashutosh Tiwari, Atul Tiwari (Eds), In the Nanomaterials in Drug Delivery, Imaging, and Tissue Engineering, John Wiley & Sons, USA, **2013**.
14. Garain, S.; Jana, S.; Sinha, T.K.; Mandal, D.; *ACS Appl. Mater. Interfaces*, **2016**, *8*, 4532. **DOI:** 10.1021/acsami.5b11356
15. Li, D.; Xia, Y.; *Adv. Mater.*, **2004**, *16*, 1151. **DOI:** 10.1002/adma.200400719
16. Lovera, D.; Bilbao, C.; Schreier, P.; Kador, L.; Schmidt, H.W.; Altstädt, V.; *Polym. Eng. Sci.*, **2009**, *49*, 2430. **DOI:** 10.1002/pen.21493
17. Doshi, J.; Reneker, D.H.; *J. Electrost.*, **1995**, *35*, 151. **DOI:** 10.1016/0304-3886(95)00041-8
18. Gregorio, R.; *J. Appl. Polym. Sci.*, **2006**, *100*, 3272. **DOI:** 10.1002/app.23137
19. Esterly, D.M.; Love, B.J.; *J. Polym. Sci., Part B: Polym. Phys.*, **2004**, *42*, 91. **DOI:** 10.1002/polb.10613
20. Damaraju, S.M.; Wu, S.; Jaffe, M.; Arinzeh, T.L.; *Biomed. Mater.*, **2013**, *8*, 045007. **DOI:** 10.1088/1748-6041/8/4/045007
21. Yee, W.A.; Kotaki, M.; Liu, Y.; Lu, X.; *Polymer*, **2007**, *48*, 512. **DOI:** 10.1016/j.polymer.2006.11.036
22. Shao, H.; Fang, J.; Wang, H.; Lang, C.; Lin, T.; *ACS Appl. Mater. Interfaces*, **2015**, *7*, 22551. **DOI:** 10.1021/acsami.5b06863
23. Gomes, J.; Nunes, J.S.; Sencadas, V.; Lanceros-Méndez, S.; *Smart Mater. Struct.*, **2010**, *19*, 065010. **DOI:** 10.1088/0964-1726/19/6/065010
24. Ribeiro, C.; Sencadas, V.; Ribelles, J.L.G.; Lanceros-Méndez, S.; *Soft Mater.*, **2010**, *8*, 274. **DOI:** 10.1080/1539445X.2010.495630
25. Liu, L.; Dzenis, Y.A.; *Nanotechnology*, **2008**, *19*, 355307. **DOI:** 10.1088/0957-4484/19/35/355307
26. Catalani, L.H.; Collins, G.; Jaffe, M.; *Macromolecules*, **2007**, *40*, 1693. **DOI:** 10.1021/ma061342d
27. Rengasamy, S.; Eimer, B.C.; Shaffer, R.E.; *Ann. Occup. Hyg.*, **2009**, *53*, 117. **DOI:** 10.1093/annhyg/men086
28. Chen, C.; Lehtimaki, M.; Willeke, K.; *AIHA J.*, **1993**, *54*, 51. **DOI:** 10.1080/15298669391354324
29. Ohmi, T.; Sudoh, S.; Mishima, H.; *IEEE Trans. Semicond. Manuf.*, **1994**, *7*, 440. **DOI:** 10.1109/66.330281
30. http://blog.gotopac.com/2010/11/18/ipa-as-a-universal-cleaner-advantages-disadvantages-2/
31. Wang, Z.L.; Chen, J.; Lin, L.; *Energy Environ. Sci.*, **2015**, *8*, 2250. **DOI:** 10.1039/C5EE01532D
32. Wang, S.; Xie, Y.; Niu, S.; Lin, L.; Liu, C.; Zhou, Y.S.; Wang, Z.L.; *Adv. Mater.*, **2014**, *26*, 6720. **DOI:** 10.1002/adma.201402491